Published in final edited form as:
Science. 2022 July 15; 377(6603): 328–335. doi:10.1126/science.abl6324.

ZAKα-driven ribotoxic stress response activates the human NLRP1 inflammasome

Kim S. Robinson[1,2], **Gee Ann Toh**[3], **Pritisha Rozario**[3], **Rae Chua**[3], **Stefan Bauernfried**[7,8], **Zijin Sun**[3], **Muhammad Jasrie Firdaus**[3], **Shima Bayat**[3], **Rhea Nadkarni**[4], **Zhi Sheng Poh**[3], **Khek Chian Tham**[2], **Cassandra R. Harapas**[5], **Chrissie K. Lim**[9,12], **Werncui Chu**[4], **Celest W. S. Tay**[3], **Kiat Yi Tan**[2], **Tianyun Zhao**[9], **Carine Bonnard**[1,2], **Radoslaw Sobota**[9], **John E. Connolly**[9], **John Common**[2], **Seth L. Masters**[5,6], **Kaiwen W. Chen**[10], **Lena Ho**[4,9], **Bin Wu**[11], **Veit Hornung**[7,8], **Franklin L. Zhong**[1,3,#]

[1]Skin Research Institute of Singapore (SRIS), #17-01 Clinical Sciences Building, 11 Mandalay Road, 308232, Singapore

[2]A*STAR Skin Research Laboratories (ASRL), A*STAR, Singapore

[3]Lee Kong Chian School of Medicine, Nanyang Technological University, 11 Mandalay Road, 308232, Singapore

[4]Cardiovascular Metabolic Disorders Program, Duke-NUS Medical School, 8 College Road, 169857, Singapore

[5]Inflammation Division, The Walter and Eliza Hall Institute of Medical Research, Parkville 3052, Australia

[6]Department of Medical Biology, University of Melbourne, Parkville, Victoria 3010, Australia

[7]Gene Center and Department of Biochemistry, Ludwig-Maximilians-Universität München, Munich, Germany

[8]Max-Planck Institute of Biochemistry, Martinsried, Germany

[9]Institute of Molecular and Cell Biology, A*STAR, Singapore

[10]Immunology Translational Research Programme and Department of Microbiology & Immunology, Yong Loo Lin School of Medicine, National University of Singapore, Singapore

[#]Lead contact. franklin.zhong@ntu.edu.sg .
[12]Present address: MiroBio Limited, Oxford, United Kingdom

Author contributions:
F.L.Z. conceived of and supervised this study. K.S.R. and G.A.T designed and performed experiments, analyzed the data, and co-wrote the manuscript, with significant contributions from P.R., S.B., Z.S., M.J.F., Z.S.P., and S.B. All co-authors contributed to writing the manuscript. S.B. performed the N/TERT constitution experiments and analyzed the data with supervision from V.H. R.C. performed the recombinant protein purification and mass spectrometry identifying phosphorylation sites with supervision from B.W., C.R.H. performed the BMDM experiments with supervision from S.L.M., and K.W.C. performed independent validation experiments with BMDMs. R.N. and W.C. performed all endothelial cell experiments with supervision from L. H., C.K.L. performed cytokine analysis with supervision from J.E.C., and C.B. and the Asian Skin Bank performed primary cell derivation and culture. K.Y.T. carried out mass spectrometry experiments with supervision from R.S.

Competing interests:
S.L.M. is a scientific advisor for Odyssey therapeutics and NRG therapeutics. J.E.C. is a member of the Board of Directors, 3T Biosciences and Chief Scientific Officer of Parker Institute for Cancer Immunotherapy. F.L.Z., K.S.R., T.G.A., S.Z. are co-inventors of a patent (PCT/SG2022/050086) based on this work.

Europe PMC Funders Author Manuscripts

[11]School of Biological Sciences, Nanyang Technological University, Singapore

Europe PMC Funders Author Manuscripts

Abstract

Human NLRP1 is an innate immune sensor predominantly expressed in the skin and airway epithelium. Here we report that human NLRP1 senses ultraviolet B (UVB)- and toxin-induced ribotoxic stress response (RSR). Biochemically, RSR leads to the direct hyperphosphorylation of a human-specific disordered linker region of NLRP1 ($NLRP1^{DR}$) by MAP3K20/ZAKα kinase and its downstream effector p38. Mutating a single ZAKα phosphorylation site in $NLRP1^{DR}$ abrogates UVB- and ribotoxin-driven pyroptosis in human keratinocytes. Moreover, fusing $NLRP1^{DR}$ to CARD8, which is insensitive to RSR by itself, creates a minimal inflammasome sensor for UVB and ribotoxins. These results provide insight into UVB sensing by human skin keratinocytes, identify several ribotoxins as NLRP1 agonists, and establish inflammasome- driven pyroptosis as an integral component of the RSR.

The innate immune system uses germline-encoded sensor proteins to recognize conserved pathogen-associated and damage-associated molecular patterns (PAMPs and DAMPs). NACHT, LRR, and PYD domain-containing proteins (NLRPs) assemble the inflammasome complex in response to intracellular pathogens or stress signals, resulting in pyroptotic cell death characterized by caspase-1 activation, GSDMD pore formation, and IL-1 secretion (1–3). Human NLRP1 is notable among inflammasome sensors due to its unusual domain arrangement and significant divergence from rodent counterparts (4–6). Inhibitors of proteases DPP8 and DPP9, such as Val-boro-Pro (VbP) (7, 8) are the only known molecules that can activate both rodent and human NLRP1, and a related human inflammasome sensor caspase activation and recruitment domain-containing protein 8 (CARD8) (9–11). Recent work has shown that human NLRP1 senses double-stranded viral RNA, viral proteases (12–14), and ultraviolet B (UVB) irradiation (15). None of these triggers activate rodent NLRP1s, which in turn sense bacterial and protozoan toxins (16–18). All known NLRP1 triggers require the proteasomal degradation of the auto-inhibitory N-terminal fragment and the oligomerization of the liberated C-terminal fragment to drive inflammasome activation (12, 19–21).

Human NLRP1 is predominantly expressed in the skin and airway epithelia (12, 22, 23). Both rare germline mutations in *NLRP1* and common *NLRP1* SNPs are associated with human skin disorders (22, 24–26). Thus, human NLRP1 plays a unique role in skin immunity. UVB radiation with wavelengths of 280-315 nm, which is responsible for acute sunburn, is the most relevant to the skin of all NLRP1 triggers identified thus far (15). However, the molecular mechanisms by which NLRP1 senses UVB are unclear.

Using the N/TERT-1 immortalized human keratinocyte cell line (hereby referred to as N/TERTs), we confirmed published findings (15, 27) that UVB irradiation causes NLRP1-dependent pyroptosis in a dose-dependent manner as measured by IL-1β secretion, GSDMD cleavage, ASC oligomerization, and rapid propidium iodide uptake (within 4-6 hours) (fig. S1, A to C and E). UVB-induced IL-1β secretion required caspase-1 activity but not NLRP3 (fig. S1, B and D). Similar to other NLRP1 activators, UVB-dependent NLRP1 activation was accompanied by a decrease in NLRP1 N-terminal fragment (NT) and was blocked

by the NEDD8/cullin inhibitor MLN4924 (figs. S1D and S2), which has been reported to regulate NLRP1-NT and CARD8-NT turnover (12, 28). Treating N/TERT cells with toxic doses of DNA-damaging chemicals, camptothecin (CPT), etoposide, and cisplatin or hydrogen peroxide failed to induce NLRP1-dependent IL-1β secretion or propidium iodide (PI) uptake at early time points (fig. S3, A and B). Thus, neither DNA damage nor oxidative damage by free radicals alone is the primary driver of UVB-induced NLRP1 inflammasome activation (Fig. 1A).

We hypothesized that UVB-driven RNA damage activates the NLRP1 inflammasome. To test this, we pretreated cells with the nucleoside analog 4-thiouridine (4-SU), which selectively sensitizes RNA to ultraviolet A (UVA) radiation. Otherwise, UVA does not cause acute damage to unmodified nucleic acids due to its lower energy (29). Only in N/TERT cells pretreated with 4-SU did UVA cause the accumulation of thymine photoadducts in the cytoplasm, which was consistent with RNA damage (fig. S3D). 4-SU+UVA induced the secretion of IL-1β (Fig. 1B and fig. S3C) and phosphorylation of stress-activated kinases (SAPKs) p38 and JNK, similar to the effects of UVB (Fig. 1B and fig. S3C). By contrast, UVA irradiation of N/TERT cells pretreated with a DNA sensitizer 5-bromo-2′-deoxyuridine (BrdU) did not induce IL-1β secretion and only effected weak SAPK phosphorylation (Fig. 1B and fig. S3C). Thus, RNA photodamage is more likely to be the upstream signal for UV-induced NLRP1 activation in keratinocytes.

Recently, the proximal sensor for UVB-triggered SAPK activation was found to be the long-splice isoform of the MAP3K20, also known as ZAKα kinase (30, 31). ZAKα senses ribosomes that have stalled and/or collided after encountering a translocation-blocking mRNA lesion, such as those induced by UVB. Activated ZAKα undergoes extensive self-phosphorylation and phosphorylates downstream SAPKs. Collectively, this pathway is termed the ribotoxic stress response (RSR) (Fig. 1A). UVB induced bona fide RSR activation in N/TERT keratinocytes marked by ZAKα, p38 and JNK phosphorylation at earlier time points and ZAKα degradation at later time points (Fig. 1B and fig. S4A). P38 and JNK phosphorylation was completely abrogated in CRISPR/Cas9 *ZAK* knockout (KO) N/TERT cells (Fig. 1B and fig. S4, B and C) after UVB or 4SU+UVA. *ZAK* KO or inhibition of ZAKα kinase activity by nilotinib blocked UVB-induced pyroptosis in N/TERT cells as measured by IL-1β secretion (Fig. 1, B and C, and fig. S4, D and E), GSDMD p30 cleavage (Fig. 1D), and rapid PI uptake (Fig. 1, E and F). Moreover, a specific ZAKα inhibitor, M443 (32) blocked UVB induced IL-1β secretion in human skin explants (fig. S4, F and G). *ZAK* KO or ZAKα inhibition did not affect VbP-driven pyroptosis in N/TERT cells (figs. S4E and S5F). Thus, ZAKα is selectively required for the NLRP1 inflammasome activation downstream of UVB. In a 293T-ASC-GFP inflammasome reporter cell line (fig. S5, A and B), full-length ZAKα induced a marked increase in ASC-GFP specks when coexpressed with NLRP1. By contrast, neither ZAKβ nor any of the ZAKα mutants defective in kinase function or sensing of ribosome stalling/collisions exhibited this function (fig. S5, C and D). Thus, the ribosome binding and RSR sensing domains of ZAKα are required for both RSR and NLRP1 inflammasome activation.

We next tested the effects of established ZAKα-activating toxins anisomycin (ANS) and doxyvinenol (DON) (Table S1) (33). Additionally, we predicted that hygromycin (HYGRO),

whose effect on ZAKα was unknown at the time of our study, would also function as a ZAKα- RSR activator. To control for protein synthesis inhibition, we tested several translational inhibitors blasticidin (BLAST), puromycin (PURO), emetine, and G418, which target different sites of the ribosome and do not activate ZAKα. A nonspecific cytotoxic drug, staurosporine (STS), was used to exclude the possibility that NLRP1 was inadvertently activated by apoptosis. ANS, DON, and HYGRO strongly induced ZAKα phosphorylation in N/TERT cells (Fig. 2A). Among the other cytotoxic drugs, only BLAST induced moderate ZAKα phosphorylation. By contrast, the level of antiapoptotic protein MCL-1, which is a sensor for translational inhibition (34), was reduced by all drugs tested (Fig. 2A). There was a correlation between the level of ZAKα phosphorylation and inflammasome activation, with ANS, HYGRO, and DON acting as strong inducers of IL-1β secretion and GSDMD p30 cleavage in N/TERT cells, and BLAST a weak inducer (Fig. 2, A and B, and fig. S5, E and F). None of the non-ZAKα activating drugs induced detectable IL-1β p17 secretion or GSDMD p30 cleavage despite significant cell death (Fig. 2, A and B). ANS also induced IL-1β and IL-18 secretion and GSDMD $p30^{+}$ cells with condensed nuclei and strong eosin staining in organotypic human skin cultures (Fig. 2, C and D). Thus, ZAKα-activating compounds, such as ANS, DON, and HYGRO are NLRP1 inflammasome activators. Moreover, this property is not caused by a general inhibition of translation.

Additionally, knocking out ZAKα, NLRP1, or components of the canonical inflammasome, but not NLRP3 or ribosome-associated protein quality control sensor, ZNF598, abrogated ANS- dependent pyroptosis in N/TERT cells (Fig. 2E and figs. S5G and S6A). ANS-dependent NLRP1 activation was also sensitive to the NEDD8/cullin inhibitor MLN4924 (fig. 6B). ANS also induced NLRP1 C-terminal fragment (CT) oligomerization and the formation of ASC-GFP specks in 293T-ASC-GFP-NLRP1 reporter cells—two established readouts for inflammasome activation—without affecting DPP9 protease activity (fig. S7, A to D). ANS could also induce inflammasome-driven pyroptosis in foreskin keratinocytes, bronchial epithelial cells, and aortic endothelial cells (fig. S8, A to E), but not in MV-4-11 cells, which employ CARD8 as the primary inflammasome sensor (fig. S8F). Thus, ZAKα activating ribotoxins, exemplified by ANS, DON, and HYGRO, function as bona fide NLRP1 activators.

We next reconstituted *NLRP1* KO N/TERT cells with human NLRP1, NLRP1ΔPYD, murine NLRP1B (muNLRP1B), or human CARD8 (Fig. 3A and fig. S9, A and B). When overexpressed, all of these heterologous sensors restored VbP-induced IL-1β secretion (Fig. 3A), as reported previously (13). By contrast, ANS only induced IL-1β in cells rescued with human NLRP1 or NLRP1ΔPYD (Fig. 3A), but not murine NLRP1 or human CARD8. Thus, ZAKα-activating molecules such as ANS are specific triggers for human NLRP1. In further support for its species specificity, ANS did not induce IL-1β release in murine bone marrow-derived macrophages (BMDMs) in an muNLRP1-dependent manner (fig. S9, C and D) (35, 36))

Human NLRP1 harbors a unique N-terminal extension encompassing the non-signaling PYD and an extended linker, which is absent in rodent NLRP1 orthologs and CARD8. This linker region is predicted to be intrinsically disordered (Fig. 3B) (37). Recent work documented a critical role of a similarly disordered linker region in CARD8 inflammasome

activation (28). We therefore tested the role of the NLRP1 linker region (a.a. 86-254, hereby termed NLRP1^{DR}). The deletion of the NLRP1^{DR}, but not NLRP1 PYD, abrogated UVB- and ANS-triggered pyroptosis (Fig. 3, A and C, and fig. S10, A and B). By contrast, VbP-dependent NLRP1 inflammasome activation was unaffected. Similar results were obtained in 293T-ASC-GFP cells (fig. S10, C and D). In addition, NLRP1^{DR} deletion attenuated NT degradation after UVB or ANS treatment (fig. S10B). Although the deletion of NLRP1^{DR} also affected VbP-induced NT degradation, NLRP1^{DR} deletion did not affect VbP-triggered pyroptosis (Fig. 3C and fig. S10B), suggesting that VbP- induced NLRP1 activation involves other domains than NLRP1^{DR}. Thus, NLRP1^{DR} is selectively required for ZAKα-dependent NLRP1 inflammasome activation.

To further dissect the function of NLRP1^{DR}, we constructed a hybrid human inflammasome sensor (termed "NLRP1^{DR}-CARD8^{ZC}" with a C-terminal FLAG tag) by fusing NLRP1^{DR} to the signaling domains of CARD8 (ZU5-UPA-CARD) (Fig. 3D). Since CARD8 itself is insensitive to UVB and ANS (Fig. 3A), any neomorphic gain in inflammasome response to ANS and UVB could be attributed to NLRP1^{DR}. When NLRP1^{DR}-CARD8^{Zc} was expressed in *NLRP1* KO N/TERTs, inflammasome activation in response to UVB (Fig. 3, E and F, and fig. S11, A and B), ANS (figs. S11C and S12, A and B), and HYGRO (fig. S11C) was restored. Thus, the disordered linker region is a necessary and sufficient determinant for NLRP1 to sense ZAKα-activating agents. NLRP1^{DR} as a GFP fusion protein (NLRP1^{DR}-GFP) showed increased fluorescence 24 hours after ANS treatment for unknown reasons (fig. S13A), suggesting that NLRP1^{DR} does not undergo proteasomal degradation and that other unknown structural elements on NLRP1 must be necessary for NT degradation.

We observed a marked band shift for NLRP1^{DR}-GFP by immunoblot whenever the cells were treated with UVB or ANS (Fig. 4A). This band shift was sensitive to post-lysis treatment with lambda phosphatase (LPP) (fig. S14A) and could be eliminated by mutating all the serine and threonine residues to alanine (a mutant hereby referred to as "Stless") (fig. S13B), which confirmed that it was caused by phosphorylated NLRP1^{DR}. PhosTag SDS-PAGE further revealed that NLRP1^{DR} was significantly phosphorylated in unstimulated cells and became further phosphorylated by ANS and UVB (Fig. 4A). We hereby refer to ANS- or UVB-dependent NLRP1^{DR} phosphorylation as hyperphosphorylation. Among all the drugs tested, only ZAKα- activating compounds could induce NLRP1^{DR} hyperphosphorylation (fig. S13C). In *ZAK*-KO N/TERT cells, ANS- and UVB-induced NLRP1^{DR} hyperphosphorylation was abrogated (Fig. 4A). ZAKα-driven NLRP1 hyperphosphorylation was specific, as ASC was not phosphorylated by ANS or VbP treatment (fig. S13D). In orthogonal experiments, coexpression of wild-type ZAKα induced a large band shift of full-length NLRP1 in 293T cells on PhosTag gel, which was diminished by the deletion of NLRP1^{DR} or the ZAKα kinase–dead mutation (p.K45A) (fig. S14, B and C). Thus, ZAKα, when activated either by overexpression or ribotoxic stress, hyperphosphorylates NLRP1 within the NLRP1^{DR}.

Mutating the serine/threonine residues to alanine within a short stretch of NLRP1^{DR} (a.a. 121-196) abrogated NLRP1 activation by UVB but did not affect VbP-driven IL-1β secretion (fig. S16). This suggested that this region harbors critical ZAKα-dependent phosphorylation sites. Recombinant ZAKα was sufficient to phosphorylate SNAP-tagged

NLRP1^{DR} purified from bacteria (Fig. 4B), indicating that NLRP1 is a direct substrate of ZAKα. Mass spectrometry of excised p-NLRP1^{DR} bands after coincubation with ZAKα identified seven distinct ZAKα phosphorylation sites. These sites are clustered in two identical motifs of the sequence PTSTAVL (Fig. 4B, and data S1), which does not exist in any other protein in the human proteome annotated in Swiss-Prot. Therefore, we propose naming this sequence the ZAKα motif. Notably, the second ZAKα motif (motif #2) falls within the crucial region (a.a. 121-196) identified by alanine scanning (fig. S16) and can be phosphorylated by ZAKα in vitro in the absence of any other phosphorylation sites (fig. S18A). Mutating the three serine/threonine residues in this motif (a.a. T178A, S179A, T180A, resulting in the NLRP1 3A mutant) eliminated UVB- and ANS-induced pyroptosis in reconstituted *NLRP1*-KO N/TERT cells, but had no effect on VbP-dependent pyroptosis (Fig. 4, D to F and fig. S17, A and B). Thus, a single phosphorylation site in the ZAKα motif within NLRP1^{DR} controls ZAKα-driven NLRP1 activation.

Given that ZAKα activates multiple SAPKs, we tested whether other kinases also contributed to ZAKα-induced NLRP1 activation. In agreement with previous results (38), multiple p38 inhibitors blocked ANS- and UVB-induced IL-1β secretion (fig. S17C) without altering VbP- dependent NLRP1 activation. By contrast, inhibitors of JNK, TAK1, SYK, and MK2 did not affect ANS-driven NLRP1 activation (fig. S17, C and D). Both p38α and p38β could phosphorylate recombinant NLRP1^{DR}, including residues within the ZAKα motifs (Fig. 4B; figs. S17F and S18, A and B; and data S1). However, p38 inhibitors showed only a modest effect on ANS-induced NLRP1^{DR} hyperphosphorylation (fig. S17E), which was completely abrogated by ZAKα inhibitors (fig. S17E). A double KO of p38α and p38β (p38α+β dKO) in N/TERTs produced a significant, but incomplete reduction of IL-1β secretion after UVB and ANS treatment (Fig. 4C and fig. S18, C and D). Thus, p38 kinases contribute to NLRP1 inflammasome activation induced by RSR inducing agents, but their roles are less critical than that of ZAKα. Since p38α and p38β are strictly downstream of ZAKα in RSR signaling, we hypothesize that ZAKα is the initiating kinase that phosphorylates NLRP1, whereas p38 kinases subsequently reinforce or amplify this response.

UVB irradiation leads to caspase-1-dependent pyroptotic cell death and IL-1β secretion in human skin keratinocytes (15, 27, 39). Initially thought to be an NLRP3-associated phenomenon, recent work has provided convincing evidence that NLRP1, instead of NLRP3, is the primary inflammasome sensor for UVB. In this work, we identify the key events controlling UVB- triggered NLRP1 inflammasome activation. By inducing cellular RNA photolesions that stall ribosomes, UVB activates the ribotoxic response (RSR) kinase ZAKα, which, together with its downstream effectors p38, phosphorylates the human-specific disordered linker region of NLRP1. A single phosphorylation site within the ZAKα motif identified here is sufficient to control NLRP1 activation in an DPP8/9-independent manner. Thus, human NLRP1 is a remarkably versatile sensor protein that can integrate multiple signals through its discrete domains. We also expand the repertoire of known human NLRP1 agonists to include multiple microbial ribotoxins, such as ANS and DON. The same results have been independently reported by a concurrent study (40). Our work also raises several questions to be addressed by future studies. For instance, it is currently unclear how ZAKα-driven hyperphosphorylation activates NLRP1 by accelerating

Europe PMC Funders Author Manuscripts

the functional degradation of NLRP1 NT. Our findings also suggest that RSR signaling may play a role in antimicrobial defense and IL-1-driven inflammation in vivo. If proven, pharmacologically targeting the ZAKα-NLRP1 axis may prove beneficial in treating human inflammatory disorders.

Supplementary Material

Refer to Web version on PubMed Central for supplementary material.

Acknowledgements

The authors would like to thank the SRIS Asian Skin Biobank (ASB), especially A. Alimat, J. Lee and A. Yap, for generating and providing human primary skin cells. We also thank the staff at NTU Optical Bio-imaging Centre and the NTU SBS Mass Spec Core Facility, especially Dr. B. Kannan and Dr. W. Meng for technical assistance with multiple experiments. The authors would also like to thank T. Nguyen for her contribution in multiple experiments. The authors are especially indebted to Prof. B. Reversade, Dr. K. Lay and Dr. S. Xue for their detailed critiques of this manuscript.

Funding

F.L.Z.'s laboratory is funded by the National Research Foundation Fellowship, Singapore (NRF-NRFF11-2019-0006) and Nanyang Assistant Professorship (NAP). K.W.C.'s laboratory acknowledges support from NUHS Internal Grant Funding (NUHSRO/2020/117/STARTUP/04). L.H.'s laboratory acknowledges funding from The National Research Foundation, Singapore (NRF-NRFF2017-05) and Howard Hughes Medical Institute (HHMI IRSP 5500873P). K.T. and J.C. are funded by IAF-PP H18/01a0/016 "Asian Skin Microbiome Program". A.S.B. is funded by Singapore's Agency for Science, Technology & Research (A*STAR) through core fund and under the IAF-PP Project (H1701a0004. Phase 2: SRIS@Novena). V.H.'s laboratory acknowledges funding from ERC-2020-ADG ENGINES (101018672). R.S. acknowledges support from A*STAR core fund. B.W. and F.L.Z. acknowledge support from NMRC-OFIRG grant from Ministry of Health, Singapore (MOH- 000382 to B.W. and F.L.Z.).

Data and materials availability

All data are available in the main text or the supplementary materials. N/TERT-1 cells were provided under a materials transfer agreement from The Brigham and Women's Hospital to Institute of Medical Biology, A*STAR.

References

1. Rathinam VAK, Fitzgerald KA. Inflammasome Complexes: Emerging Mechanisms and Effector Functions. Cell. 2016; 165: 792–800. [PubMed: 27153493]
2. Broz P, Dixit VM. Inflammasomes: mechanism of assembly, regulation and signalling. Nat Rev Immunol. 2016; 16: 407–420. [PubMed: 27291964]
3. Man SM, Kanneganti T-D. Regulation of inflammasome activation. Immunol Rev. 2015; 265: 6–21. [PubMed: 25879280]
4. Taabazuing CY, Griswold AR, Bachovchin DA. The NLRP1 and CARD8 inflammasomes. Immunol Rev. 2020; 297: 13–25. [PubMed: 32558991]
5. Bachovchin DA. NLRP1: a jack of all trades, or a master of one? Mol Cell. 2021; 81: 423–425. [PubMed: 33545058]
6. Mitchell PS, Sandstrom A, Vance RE. The NLRP1 inflammasome: new mechanistic insights and unresolved mysteries. Curr Opin Immunol. 2019; 60: 37–45. [PubMed: 31121538]
7. Zhong FL, Robinson K, Teo DET, Tan K-Y, Lim C, Harapas CR, Yu C-H, Xie WH, Sobota RM, Au VB, Hopkins R, et al. Human DPP9 represses NLRP1 inflammasome and protects against autoinflammatory diseases via both peptidase activity and FIIND domain binding. J Biol Chem. 2018; 293: 18864–18878. [PubMed: 30291141]

8. Okondo MC, Rao SD, Taabazuing CY, Chui AJ, Poplawski SE, Johnson DC, Bachovchin DA. Inhibition of Dpp8/9 Activates the Nlrp1b Inflammasome. Cell Chem Biol. 2018; 25: 262–267. e5 [PubMed: 29396289]

9. Johnson DC, Taabazuing CY, Okondo MC, Chui AJ, Rao SD, Brown FC, Reed C, Peguero E, de Stanchina E, Kentsis A, Bachovchin DA. DPP8/DPP9 inhibitor-induced pyroptosis for treatment of acute myeloid leukemia. Nat Med. 2018; 24: 1151–1156. [PubMed: 29967349]

10. Hollingsworth LR, Sharif H, Griswold AR, Fontana P, Mintseris J, Dagbay KB, Paulo JA, Gygi SP, Bachovchin DA, Wu H. DPP9 sequesters the C terminus of NLRP1 to repress inflammasome activation. Nature. 2021; 592: 778–783. [PubMed: 33731932]

11. Huang M, Zhang X, Toh GA, Gong Q, Wang J, Han Z, Wu B, Zhong F, Chai J. Structural and biochemical mechanisms of NLRP1 inhibition by DPP9. Nature. 2021; 592: 773–777. [PubMed: 33731929]

12. Robinson KS, Teo DET, Tan KS, Toh GA, Ong HH, Lim CK, Lay K, Au BV, Lew TS, Chu JJH, Chow VTK, et al. Enteroviral 3C protease activates the human NLRP1 inflammasome in airway epithelia. Science. 2020; 370 doi: 10.1126/science.aay2002

13. Bauernfried S, Scherr MJ, Pichlmair A, Duderstadt KE, Hornung V. Human NLRP1 is a sensor for double-stranded RNA. Science. 2021; 371 doi: 10.1126/science.abd0811

14. Tsu BV, Beierschmitt C, Ryan AP, Agarwal R, Mitchell PS, Daugherty MD. Diverse viral proteases activate the NLRP1 inflammasome. Elife. 2021; 10 doi: 10.7554/eLife.60609

15. Fenini G, Grossi S, Contassot E, Biedermann T, Reichmann E, French LE, Beer H-D. Genome Editing of Human Primary Keratinocytes by CRISPR/Cas9 Reveals an Essential Role of the NLRP1 Inflammasome in UVB Sensing. J Invest Dermatol. 2018; 138: 2644–2652. [PubMed: 30096351]

16. Cirelli KM, Gorfu G, Hassan MA, Printz M, Crown D, Leppla SH, Grigg ME, Saeij JPJ, Moayeri M. Inflammasome sensor NLRP1 controls rat macrophage susceptibility to Toxoplasma gondii. PLoS Pathog. 2014; 10 e1003927 [PubMed: 24626226]

17. Chavarría-Smith J, Vance RE. Direct proteolytic cleavage of NLRP1B is necessary and sufficient for inflammasome activation by anthrax lethal factor. PLoS Pathog. 2013; 9 e1003452 [PubMed: 23818853]

18. Ewald SE, Chavarria-Smith J, Boothroyd Jc. NLRP1 is an inflammasome sensor for Toxoplasma gondii. Infect Immun. 2014; 82: 460–468. [PubMed: 24218483]

19. Sandstrom A, Mitchell PS, Goers L, Mu EW, Lesser CF, Vance RE. Functional degradation: A mechanism of NLRP1 inflammasome activation by diverse pathogen enzymes. Science. 2019; 364 doi: 10.1126/science.aau1330

20. Chui AJ, Okondo MC, Rao SD, Gai K, Griswold AR, Johnson DC, Ball DP, Taabazuing CY, Orth EL, Vittimberga BA, Bachovchin DA. N-terminal degradation activates the NLRP1B inflammasome. Science. 2019; 364: 82–85. [PubMed: 30872531]

21. Xu H, Shi J, Gao H, Liu Y, Yang Z, Shao F, Dong N. The N-end rule ubiquitin ligase UBR2 mediates NLRP1B inflammasome activation by anthrax lethal toxin. EMBO J. 2019; 38 e101996 [PubMed: 31268597]

22. Zhong FL, Mamaï O, Sborgi L, Boussofara L, Hopkins R, Robinson K, Szeverényi I, Takeichi T, Balaji R, Lau A, Tye H, et al. Germline NLRP1 Mutations Cause Skin Inflammatory and cancer Susceptibility Syndromes via Inflammasome Activation. Cell. 2016; 167: 187–202. e17 [PubMed: 27662089]

23. Sand J, Haertel E, Biedermann T, Contassot E, Reichmann E, French LE, Werner S, Beer H-D. Expression of inflammasome proteins and inflammasome activation occurs in human, but not in murine keratinocytes. Cell Death Dis. 2018; 9: 24. [PubMed: 29348630]

24. Drutman SB, Haerynck F, Zhong FL, Hum D, Hernandez NJ, Belkaya S, Rapaport F, de Jong SJ, Creytens D, Tavernier SJ, Bonte K, et al. Homozygous NLRP1 gain-of-function mutation in siblings with a syndromic form of recurrent respiratory papillomatosis. Proc Natl Acad Sci U S A. 2019; 116: 19055–19063. [PubMed: 31484767]

25. Grandemange S, Sanchez E, Louis-Plence P, TranMau-Them F, Bessis D, Coubes C, Frouin E, Seyger M, Girard M, Puechberty J, Costes V, et al. A new autoinflammatory and autoimmune

Europe PMC Funders Author Manuscripts

syndrome associated with NLRP1 mutations: NAIAD (NLRP1-associated autoinflammation with arthritis and dyskeratosis). Ann Rheum Dis. 2017; 76: 1191–1198. [PubMed: 27965258]

26. Levandowski CB, Mailloux CM, Ferrara TM, Gowan K, Ben S, Jin Y, McFann KK, Holland PJ, Fain PR, Dinarello CA, Spritz RA. NLRP1 haplotypes associated with vitiligo and autoimmunity increase interleukin-1β processing via the NLRP1 inflammasome. Proc Natl Acad Sci U S A. 2013; 110: 2952–2956. [PubMed: 23382179]
27. Sollberger G, Strittmatter GE, Grossi S, Garstkiewicz M, auf dem Keller U, French LE, Beer H-D. Caspase-1 Activity Is Required for UVB-Induced Apoptosis of Human Keratinocytes. J Invest Dermatol. 2015; 135: 1395–1404. [PubMed: 25562666]
28. Chui AJ, Griswold AR, Taabazuing CY, Orth EL, Gai K, Rao SD, Ball DP, Hsiao JC, Bachovchin DA. Activation of the CARD8 Inflammasome Requires a Disordered Region. Cell Rep. 2020; 33 108264 [PubMed: 33053349]
29. Karran P, Brem R. Protein oxidation, UVA and human DNA repair. DNA Repair. 2016; 44: 178–185. [PubMed: 27324272]
30. Vind AC, Snieckute G, Blasius M, Tiedje C, Krogh N, Bekker-Jensen DB, Andersen KL, Nordgaard C, Tollenaere MAX, Lund AH, Olsen JV, et al. ZAKα Recognizes Stalled Ribosomes through Partially Redundant Sensor Domains. Mol Cell. 2020; 78: 700–713. e7 [PubMed: 32289254]
31. Wu CC-C, Peterson A, Zinshteyn B, Regot S, Green R. Ribosome Collisions Trigger General Stress Responses to Regulate Cell Fate. Cell. 2020; 182: 404–416. e14 [PubMed: 32610081]
32. Markowitz D, Powell C, Tran NL, Berens ME, Ryken TC, Vanan M, Rosen L, He M, Sun S, Symons M, Al-Abed Y, et al. Pharmacological Inhibition of the Protein Kinase MRK/ZAK Radiosensitizes Medulloblastoma. Mol Cancer Ther. 2016; 15: 1799–1808. [PubMed: 27207779]
33. Vind AC, Genzor AV, Bekker-Jensen S. Ribosomal stress-surveillance: three pathways is a magic number. Nucleic Acids Res. 2020; 48: 10648–10661. [PubMed: 32941609]
34. Orzalli MH, Prochera A, Payne L, Smith A, Garlick JA, Kagan JC. Virus-mediated inactivation of anti-apoptotic Bcl-2 family members promotes Gasdermin-E-dependent pyroptosis in barrier epithelial cells. Immunity. 2021; doi: 10.1016/j.immuni.2021.04.012
35. Vyleta ML, Wong J, Magun BE. Suppression of ribosomal function triggers innate immune signaling through activation of the NLRP3 inflammasome. PLoS One. 2012; 7 e36044 [PubMed: 22606244]
36. Briard B, Fontaine T, Samir P, Place DE, Muszkieta L, Malireddi RKS, Karki R, Christgen S, Bomme P, Vogel P, Beau R, et al. Galactosaminogalactan activates the inflammasome to provide host protection. Nature. 2020; 588: 688–692. [PubMed: 33268895]
37. Hanson J, Paliwal KK, Litfin T, Zhou Y. SPOT-Disorder2: Improved Protein Intrinsic Disorder Prediction by Ensembled Deep Learning. Genomics Proteomics Bioinformatics. 2019; 17: 645–656. [PubMed: 32173600]
38. Fenini G, Grossi S, Gehrke S, Beer H-D, Satoh TK, Contassot E, French LE. The p38 Mitogen-Activated Protein Kinase Critically Regulates Human Keratinocyte Inflammasome Activation. J Invest Dermatol. 2018; 138: 1380–1390. [PubMed: 29287762]
39. Feldmeyer L, Keller M, Niklaus G, Hohl D, Werner S, Beer H-D. The Inflammasome Mediates UVB-Induced Activation and Secretion of Interleukin-1β by Keratinocytes. Curr Biol. 2007; 17: 1140–1145. [PubMed: 17600714]
40. Jenster L, Lange K, Normann S, vom Hemdt A, Wuerth JD, Schiffelers LD, Tesfamariam YM, Gohr FN, Klein L, Kaltheuner IH. P38 kinases mediate NLRP1 inflammasome activation after ribotoxic stress response and virus infection. 2022. available at https://europepmc.org/article/ppr/ppr446691

Europe PMC Funders Author Manuscripts

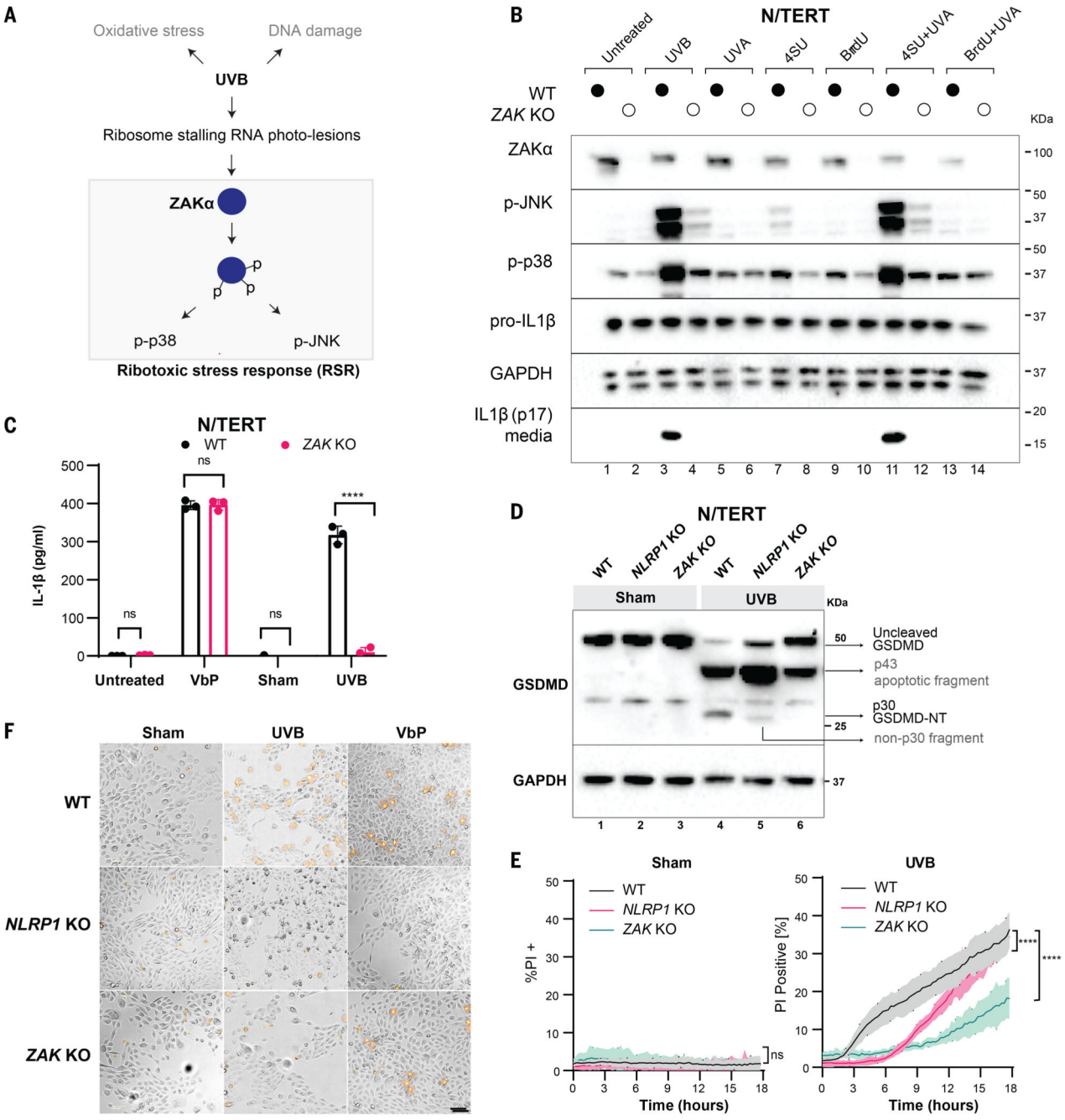

Figure 1. ZAKα is required for UVB-triggered NLRP1 inflammasome activation.

(**A**) Schematic indicating types of cellular damage caused by UVB irradiation. UVB activates ribotoxic stress response (RSR) signaling through ZAKα. (**B**) Immunoblot of WT N/TERT cells or *ZAK KO* (sg4) N/TERT cells treated with the indicated combinations of photosensitizer (10 μM) for 4 hours with or without UVA. UVB (100 mJ/cm^2) was used as a positive control. *, residual signal after membrane stripping. (**C**) IL-1β ELISA of WT or *ZAK KO* (sg4) N/TERT cells after VbP (3 μM) treatment, sham or UVB (100 mJ/cm^2) irradiation. Cell culture media were collected 24 hours later. (**D**) GSDMD immunoblot of

Europe PMC Funders Author Manuscripts

WT, *NLRP1* KO, *ZAK KO* (sg4) N/TERT cells treated with UVB (100 mJ/cm^2) or sham-irradiated. Cell lysates were harvested 24 hours later. Different GSDMD cleavage fragments are shown by black arrows. Note that the GSDMD antibody used in this experiment recognizes all GSDMD-cleaved products. In *NLRP1* KO cells UVB leads to a weak band <30 kDa. (**E**) Quantification of the percentage of PI-positive WT, *NLRP1* KO, *ZAK KO* (sg4) N/TERT cells after sham or UVB (100 mJ/cm^2) irradiation. (**F**) Representative images of PI inclusion 5 hours post irradiation from 3 independent experiments. Scale bar represents 100 μm. Error bars represent standard errors of the mean (S.E.M.) from three biological replicates, where one replicate refers to an independent seeding and treatment of the cells. The significance values were calculated based on two-way ANOVA followed by Sidak's test for multiple pairwise comparisons in (**C**), and two-tailed Kolmogorov-Smirnov test at 95% confidence interval in (**E**). ns, non-significant, **** $P<0.0001$.

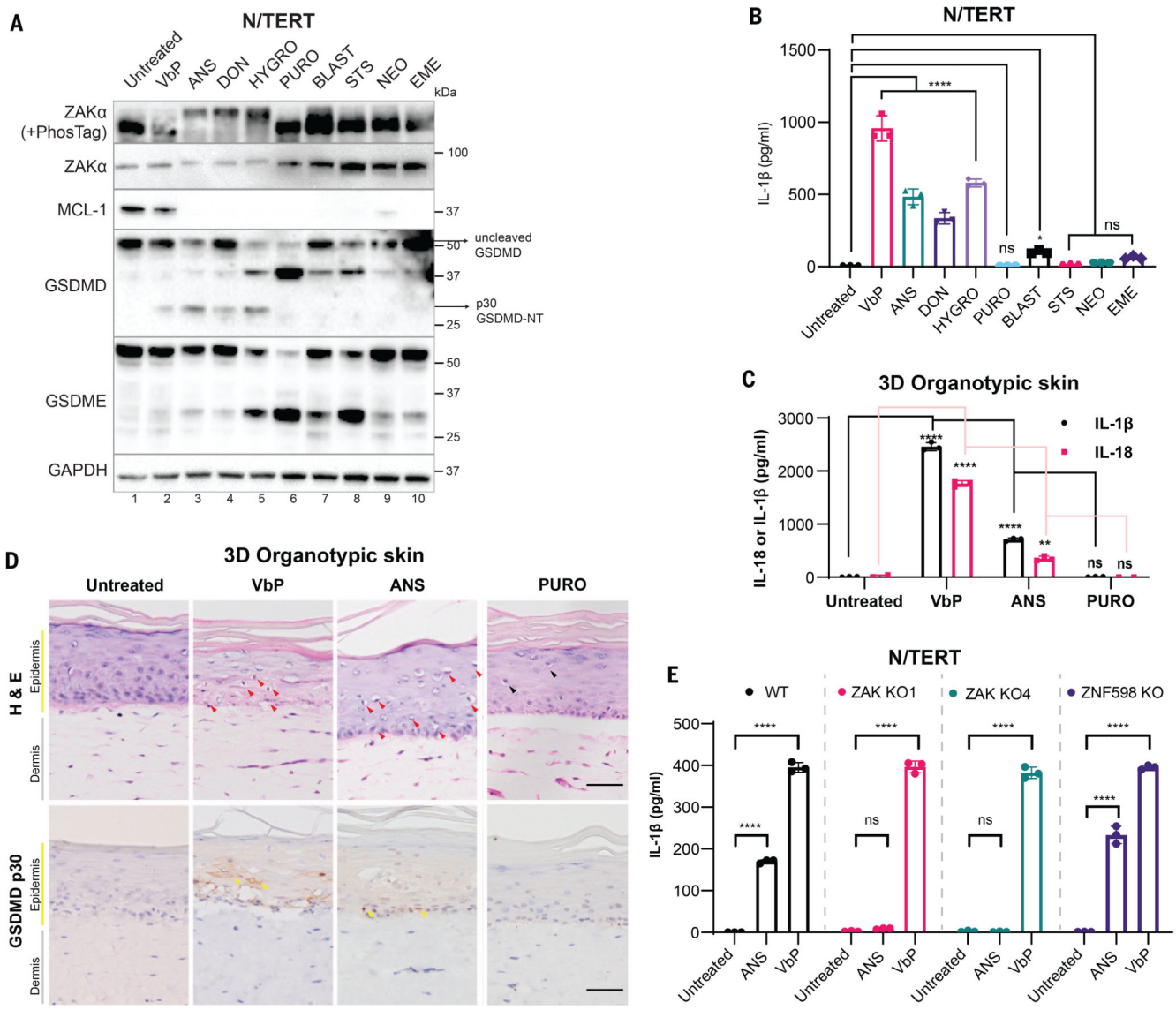

Figure 2. ZAKα-activating compounds induce NLRP1-driven pyroptosis.

(**A**) Immunoblot of N/TERT cell lysate after treatment with the indicated drugs. ZAKα phosphorylation was detected after 3 hours of drug treatment, while immunoblots for MCL-1, GSDMD, and GSDME were performed using samples 24 hours post treatment. (**B**) IL-1β ELISA of N/TERT cell media 24 hours post treatment with the indicated drugs at concentrations specified in A. Note that a smaller volume of the media and a higher number of cells were used in this experiment, accounting for the overall higher concentration of IL-1β. (**C**) IL-1β and IL-18 ELISA of growth media collected from 3D organotypic skin cultures treated with the indicated drugs. (**D**) H&E and cleaved GSDMD-NT (p30 specific) immunostaining of 3D organotypic skin cultures treated with the indicated drugs in D. Scale bar represents 100 μm. Red arrows indicate keratinocytes with diminished eosin but dense hematoxylin staining that were abundant in VbP- and ANS-treated cultures. Black arrows indicate putatively apoptotic cells with low eosin and hematoxylin staining that

Europe PMC Funders Author Manuscripts

were abundant in PURO-treated samples. Yellow arrows indicate membranous GSDMD p30 staining. Images represent one of 3 independent organotypic skin cultures. (**E**) IL-1β ELISA of culture media from N/TERT cells of the indicated genotypes after 24 hours of drug treatment. VbP was used at 3 μM and ANS at 1 μM. Error bars represent standard errors of the mean (S.E.M.) from three biological replicate experiments, where one replicate refers to an independent seeding and treatment of the cells. The significance values were calculated based on two-way ANOVA followed by Dunnett's test for multiple pairwise comparisons in (**B**) and (**C**), and Sidak's test in (**E**). ns, non-significant, *P<0.05, **P<0.01, ****P<0.0001.

Europe PMC Funders Author Manuscripts

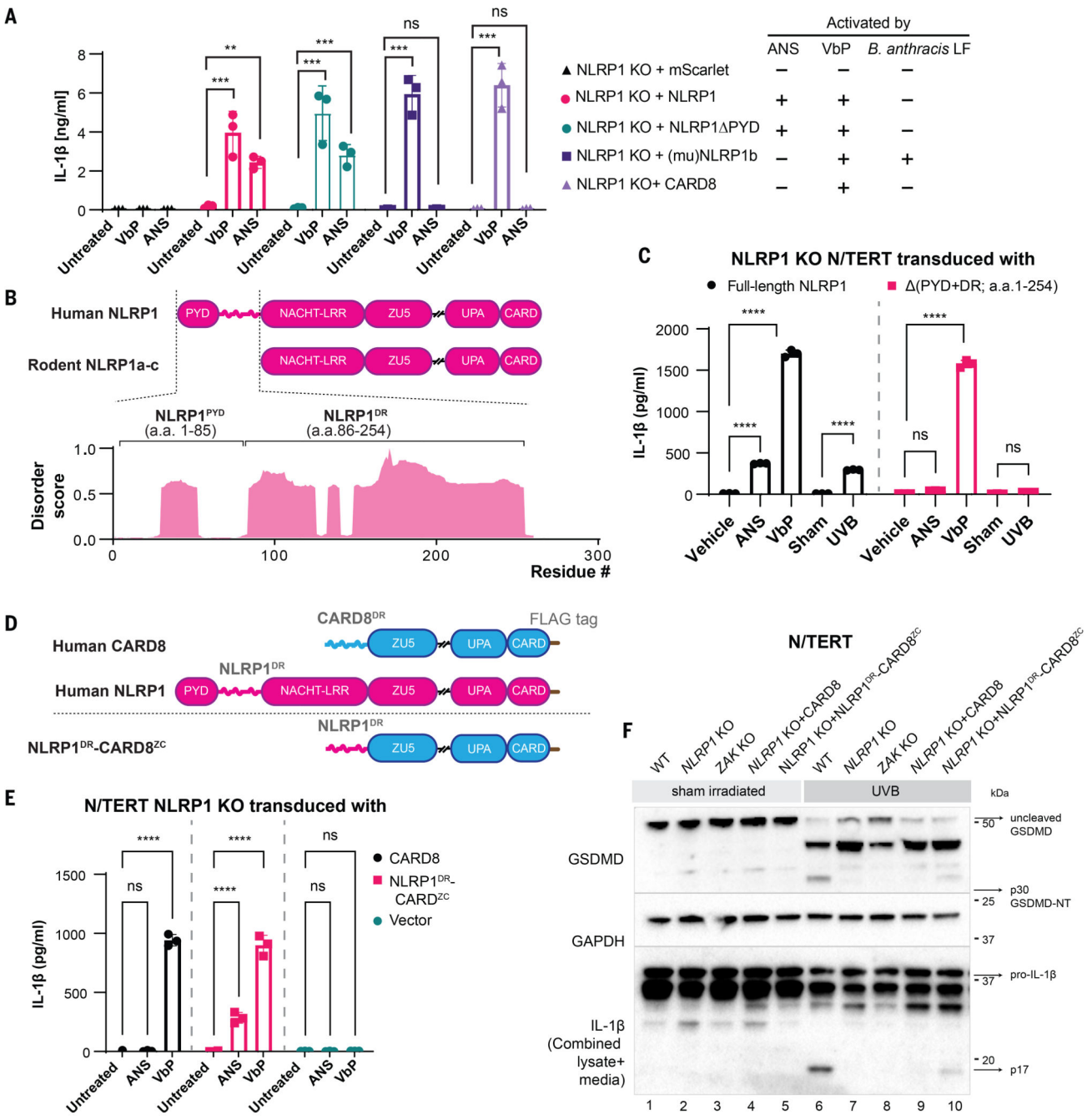

Figure 3. A disordered linker region of human NLRP1 selectively mediates ZAKα-dependent activation.

(**A**) IL-1β ELISA from *NLRP1* KO N/TERT cells reconstituted with the indicated NLRP1 variants and CARD8 treated with ANS (1 μM) and VbP (3 μM). Note that this experiment was performed independently using higher cell numbers. (**B**) Comparison between the domain structures of human NLRP1 and rodent NLRP1a-c. The predicted disorder score was calculated for a.a. 1-300 of human NLRP1. (**C**) IL-1β ELISA from *NLRP1*-KO N/TERT cells reconstituted with GFP-full-length NLRP1 or NLRP1 lacking PYD+DR

Europe PMC Funders Author Manuscripts

Europe PMC Funders Author Manuscripts

(a.a.1-254). Cells were treated with the indicated drugs, or sham- or UVB-irradiated and harvested 24 hours post-treatment. (**D**) Comparison of the domain arrangements of human NLRP1 and CARD8 and the engineered hybrid sensor referred to as NLRP1^{DR}-CARD8^{ZC}. (**E**) IL-1β ELISA from *NLRP1*-KO N/TERT cells transduced with CARD8 or NLRP1^{DR}-CARD8^{ZC} and treated with 1 μM ANS or 3 μM VbP for 24 hours. (**F**) GSDMD and IL-1β immunoblot from the cells in E, along with WT or *ZAK* KO N/TERT cells irradiated with UVB. The GSDMD antibody recognizes both full-length and cleaved forms, including p43 and p30. The IL-1β immunoblot was performed with samples that combined lysate and 10 times concentrated media. The error bars represent standard errors of the mean (S.E.M.) from three biological replicates, where one replicate refers to an independent seeding and treatment of the cells. The significance values in (**A**), (**C**) and (**E**) were calculated based on two-way ANOVA followed by Sidak's test for multiple pairwise comparisons. Significance values were indicated as: ns, non-significant, ** $P<0.01$, *** $P<0.001$, **** $P<0.0001$.

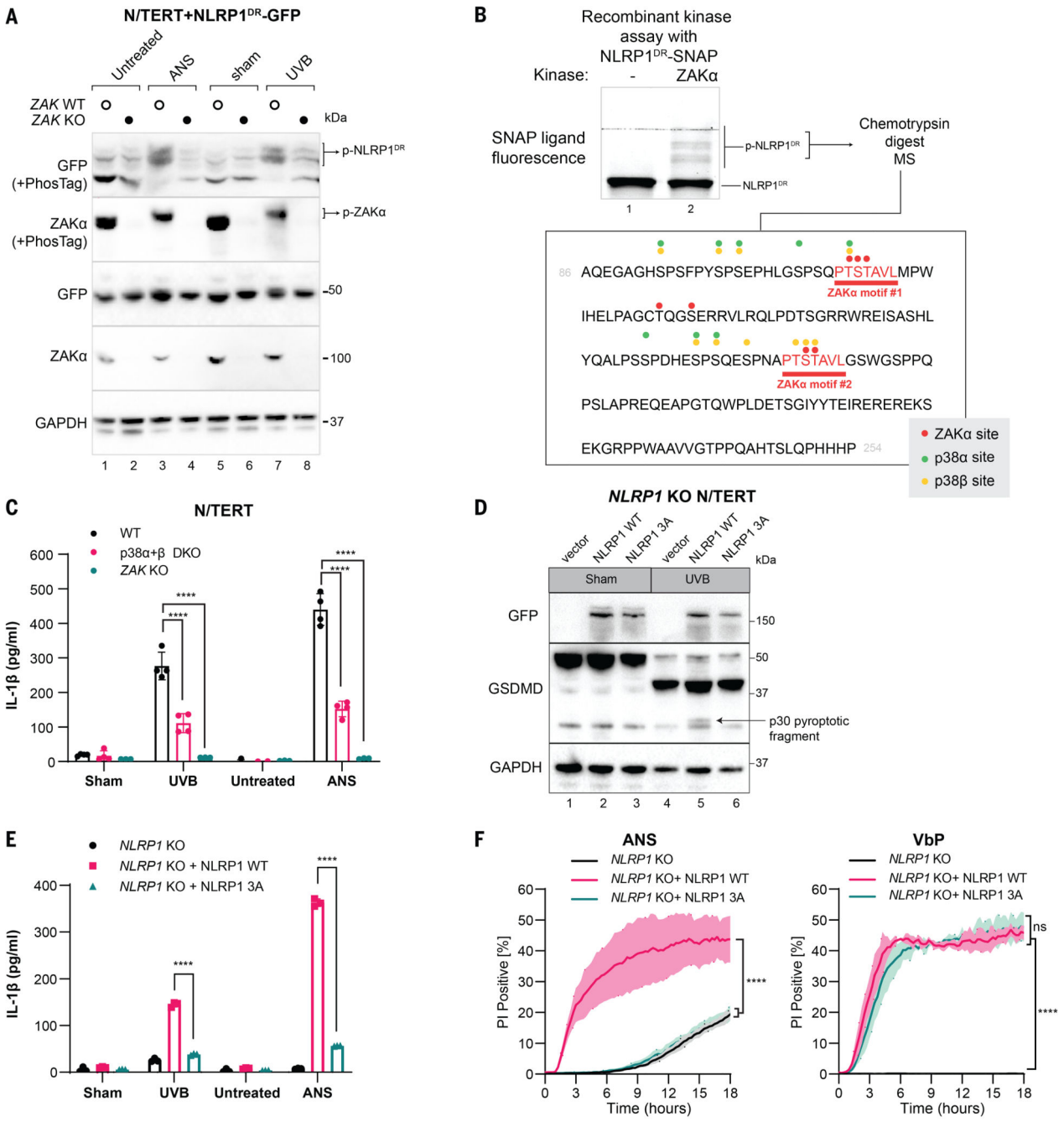

Figure 4. Hyperphosphorylation of NLRP1^{DR} by ZAKα and p38 activates NLRP1.

(**A**) Immunoblot following SDS-PAGE or PhosTag SDS-PAGE of wild-type or *ZAK*-KO N/TERT cells expressing NLRP1^{DR}-GFP. Cells were harvested 2 hours post ANS treatment or UVB irradiation. (**B**) Recombinant SNAP-tagged NLRP1^{DR} was incubated with recombinant ZAKα in a standard kinase reaction for 30 min. NLRP1^{DR} phosphorylation was visualized with SNAP ligand fluorescence (TMR) on a PhosTag-containing SDS-PAGE gel. (**C**) IL-1β ELISA from WT, *MAPK14 MAPK11* DKO (denoted as p38α+β DKO) and *ZAK* KO N/TERT cells 24 hours after UVB irradiation or ANS treatment. (**D**) GFP

Europe PMC Funders Author Manuscripts

and GSDMD immunoblot of *NLRP1*-KO N/TERT cells expressing full-length WT NLRP1 or full-length NLRP1 T178A, S179A, T180A (3A) mutant after UVB irradiation. All constructs were fused with GFP at the N- terminus. GSDMD p30 is marked with a black arrow. Cells were harvested 24 hours post UVB treatment. (**E**) IL-1β ELISA from *NLRP1*-KO N/TERT cells expressing full length WT NLRP1 or full-length NLRP1 T178A, S179A, T180A (3A) mutant 24 hours after UVB irradiation or ANS treatment. (**F**) Quantification of the percentage of PI+ *NLRP1*-KO N/TERT cells expressing full-length WT NLRP1 or full-length NLRP1 T178A, S179A, T180A (3A) mutants in the presence of ANS or VbP. Images were acquired at 15-min intervals for 18 hours. Error bars represent standard errors of the mean (S.E.M.) from three biological replicates, where one replicate refers to an independent seeding and treatment of the cells. The significance values were calculated based on two-way ANOVA followed by Sidak's test for multiple pairwise comparisons in (**C**) and (**E**), and two-tailed Kolmogorov-Smirnov test at 95% confidence interval in (**F**). ns, non-significant, ****$P<0.0001$.

Europe PMC Funders Author Manuscripts